Bandwidth Programmable Optical Nyquist Pulse Generation In Passively Mode-Locked Fiber Laser

Sonia Boscolo,[1,*] **Christophe Finot,**[2] **Sergei K. Turitsyn**[1]

[1]*Aston Institute of Photonic Technologies, School of Engineering and Applied Science, Aston University, Birmingham B4 7ET, United Kingdom*
[2]*Laboratoire Interdisciplinaire Carnot de Bourgogne, UMR 6303 CNRS-Université de Bourgogne/Franche-Comtè, 9 avenue Alain Savary, BP 47870, 21078, Dijon Cedex, France*
[*]*Corresponding author: s.a.boscolo@aston.ac.uk*

DOI: 10.1109/JPHOT.2015.XXXXXXX

Abstract: We propose and numerically demonstrate a novel, simple method to produce optical Nyquist pulses based on pulse shaping in a passively mode-locked fiber laser with an in-cavity flat-top spectral filter. The proposed scheme takes advantage of the nonlinear in-cavity dynamics of the laser, and offers the possibility to generate high-quality sinc-shaped pulses with widely tunable bandwidth directly from the laser oscillator. We also show that the use of a filter with a corrective convex profile relaxes the need for large nonlinear phase accumulation in the cavity by offsetting the concavity of the nonlinearly broadened pulse spectrum.

Index Terms: Mode-locked fiber lasers, pulse shaping, frequency filtering, nonlinear fiber optics.

1. Introduction

Sinc-shaped Nyquist pulses in the time domain possess a rectangular spectrum, enabling bandwidth efficient encoding of data and intrinsically satisfying the Nyquist criterion for zero intersymbol interference (see, e.g., [1], [2] and references therein). These temporal and spectral properties are of key interest for high-capacity optical communication systems and various other applications. For example, sinc pulses can provide substantial performance improvement to optical sampling devices [3] because their waveform corresponds to the ideal interpolation function for the perfect restoration of band-limited signals from discrete and noisy data [4]. Furthermore, the spectral features of sinc pulses could enable the implementation of ideal rectangular microwave photonics filters [5] with tunable passband profiles, thus providing interesting possibilities for all-optical signal processing [6], spectroscopy [7], and light storage [8].

These attractive properties stimulated a great deal of research activity in the field of optical Nyquist pulse transmission and generation. Various optical methods have been reported, including spectral reshaping of mode-locked laser [9] or fiber optical parametric amplification pumped by parabolic pulses in combination with a phase modulator to compensate the pump-induced chirp [10]. Additionally, sequences of very high-quality sinc-shaped pulses were produced by the direct synthesis of a flat phase-locked frequency comb using two cascaded Mach Zehnder modulators [11]. An extension of this scheme, including an additional nonlinear optical stage based on four-wave mixing, was proposed in [12] to expand the bandwidth of the generated comb beyond the limit imposed by the electronic bandwidth of the modulators. Furthermore, a Nyquist laser that can

directly emit an optical Nyquist pulse train was recently demonstrated [13]. In the laser design demonstrated in [13], the generation of Nyquist pulses is made possible by a combination of parabolic time-domain shaping at the pulse peak with an optical intensity modulator and spectral-domain shaping on the pulse wings with a spectral filter. In general, the concept of an in-cavity spectral pulse shaper has been proved to have great potential for controlling the dynamics and the output of mode-locked fiber lasers [14], [15], [16], while obviously entailing a more power efficient technique than pulse shaping implemented through direct filtering of a laser output.

In this paper, we propose a novel, simple approach to the design of a Nyquist laser, which relies on nonlinear in-cavity pulse dynamics and pulse shaping by an in-cavity flat-top spectral filter in a passively mode-locked fiber laser. An improved approach, based on the use of a filter's profile with a corrective convex top, is also proposed to compensate for the concavity of the pulse spectrum obtained after nonlinear expansion in the fiber. The need for large nonlinear phase accumulation in the fiber is thereby relaxed. We numerically show the possibility to achieve sinc-shaped Nyquist pulses of high quality and widely tunable bandwidth with the proposed scheme.

2. Laser Configuration And Numerical Model

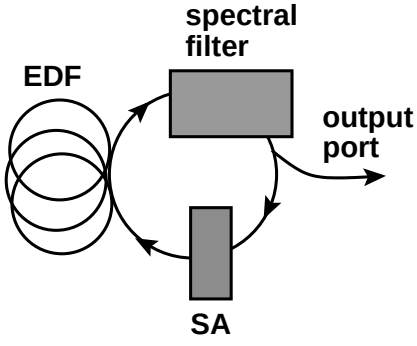

Fig. 1. Schematic of the laser. EDF: erbium-doped fiber; SA: saturable absorber.

The cavity configuration considered is a simple ring cavity as shown in Fig. 1. The laser consists of a 1 m-long segment of erbium-doped fiber (EDF) with normal group-velocity dispersion (GVD), which acts as the gain and nonlinear element of the cavity, followed by a spectral filter, which realizes the pulse shaping, and a saturable absorber (SA) element. Pulse propagation within the fiber section is modeled with a standard modified nonlinear Schrödinger equation for the slowly-varying pulse envelope:

$$i\psi_z - \frac{1}{2}\beta_2\psi_{tt} + \gamma|\psi|^2\psi = \frac{i}{2}g\left(\psi + \frac{1}{\Omega^2}\psi_{tt}\right), \tag{1}$$

where $\beta_2 = 25\,\mathrm{fs}^2/\mathrm{mm}$ is the GVD parameter and $\gamma = 0.005\,(\mathrm{W\,m})^{-1}$ is the coefficient of cubic nonlinearity of the fiber [17]. The dissipative terms on the right-hand side of Eq. (1) represent linear gain as well as a parabolic approximation to the gain profile with the bandwidth Ω corresponding to 40 nm full-width at half-maximum (FWHM) bandwidth. The gain is saturated according to $g = g_0/(1 + W/W_0)$, where $g_0 = 30\,\mathrm{dB/m}$ is the small-signal gain, $W = \int \mathrm{d}t\,|\psi|^2$ is the pulse energy, and $W_0 = 150\,\mathrm{pJ}$ is the gain saturation energy. The SA is given by a monotonically increasing transfer function $T = 1 - q_0/[1 + P(t)/P_0]$, where $q_0 = 0.9$ is the unsaturated loss, $P(t)$ is the instantaneous pulse power, and $P_0 = 150\,\mathrm{W}$ is the saturation power. The filter is modeled by the spectral response $H(f) = R(f)\exp\left[i\beta_{2,\mathrm{acc}}(2\pi f)^2/2\right]$, where $R(f)$ is a spectral profile with sharply

decaying edges outside its bandwidth and a Gaussian top, given by

$$R(f) = \begin{cases} \frac{\tau_p}{2} \exp\left(\alpha f^2\right), & |f| < \frac{1}{\tau_p} \\ \frac{\tau_p}{4}, & |f| = \frac{1}{\tau_p} \\ 0 & \text{otherwise} \end{cases} \tag{2}$$

where $B = 2/\tau_p$ is the spectral bandwidth (defined as the width of both edges of the spectrum tail), τ_p is the time interval between zero crossings of the corresponding sinc-function-like impulse response, and α is an adjustable parameter defining the width and concavity of the spectrum top. Note that it is customary to include a non-unit peak amplitude in the frequency-domain description of the filter in order to give the impulse response in terms of the normalised sinc function. However, in our numerical simulations we applied the normalised filter's response to the Fourier transform of the pulse. Note also that approximating the Gaussian function by the first two terms of its Taylor series, that is, by a quadratic function, in the filter's response would yield similar results to those presented hereafter. For the special value $\alpha = 0$, $R(f)$ is the rectangular spectral profile associated with the Nyquist sinc-function impulse response [1], [9]

$$r(t) = \frac{\sin(2\pi t/\tau_p)}{2\pi t/\tau_p}, \tag{3}$$

while $\alpha > 0$ ($\alpha < 0$) yields a convex or inverted (concave or conventional) Gaussian top. A variety of filters with very steep edges and adjustable bandwidth are readily available. The corrective Gaussian-top profile can be provided by a programmable liquid crystal on silicon optical processor, the shape and bandwidth of which can be software configured [18]; such devices are already commercially available. Note that optimization of the filter's profile is relatively easy as it requires adjustment of only one parameter (α). An additional parabolic spectral phase filter can be included into the pulse shaper to add a specific amount of GVD $\beta_{2,\mathrm{acc}}$ (in ps^2) to the cavity and, thus, control the net cavity dispersion [16]. The output of the laser is monitored behind a 70% coupler at the output of the pulse shaper. The numerical model is solved with a standard symmetric split-step propagation algorithm, and the initial field is a picosecond Gaussian temporal profile.

3. In-Cavity Nyquist Pulse Shaping

The pulse solutions obtained for a flat-top spectral profile ($\alpha = 0$) applied to the filter with related zero-crossing pulse durations of 2.5 ps, 1 ps and 0.5 ps are shown in Fig. 2, and compared with the solutions obtained with a convex Gaussian-top profile. The shape correction factor α was optimized for each pulse duration, and no in-cavity dispersion control was used in these simulations. It is seen that the use of the basic rectangular shape for the filter's spectral response already allows us to obtain sinc-shaped pulses at the output of the laser that coincide well with the theoretical ones described by (3), and feature a spectrum that is fairly close to the ideal rectangular case. When a convex spectral profile is applied to the filter, the correction of the non perfectly flattened pulse spectrum after the gain fiber by the filter brings about sinc pulses of enhanced quality and with an almost ideal rectangular spectrum at the laser output for all the pulse durations being considered.

An example of pulse evolution when the basic rectangular filtering method is employed is illustrated in Fig. 3 by plots of the FWHM pulse duration and spectral bandwidth as functions of position in the cavity. It is seen that both the temporal and spectral widths of the pulse increase in the gain fiber as the pulse acquires a positive (normal) instantaneous frequency shift or chirp. The initial slight decrease of the bandwidth originates from the reshaping of the spectrum from a rectangular-like profile at the entrance of the fiber to a parabolic-like shape near the peak with a transition to a steep decay in the first stage of evolution in the fiber. After this stage, the spectrum broadens significantly, and eventually develops the steep and structured edges characteristic of self-phase modulation (SPM). The filter and SA reverse these changes. The filter compensates for spectral and part of temporal broadening, and cancels the temporal phase accumulation in the

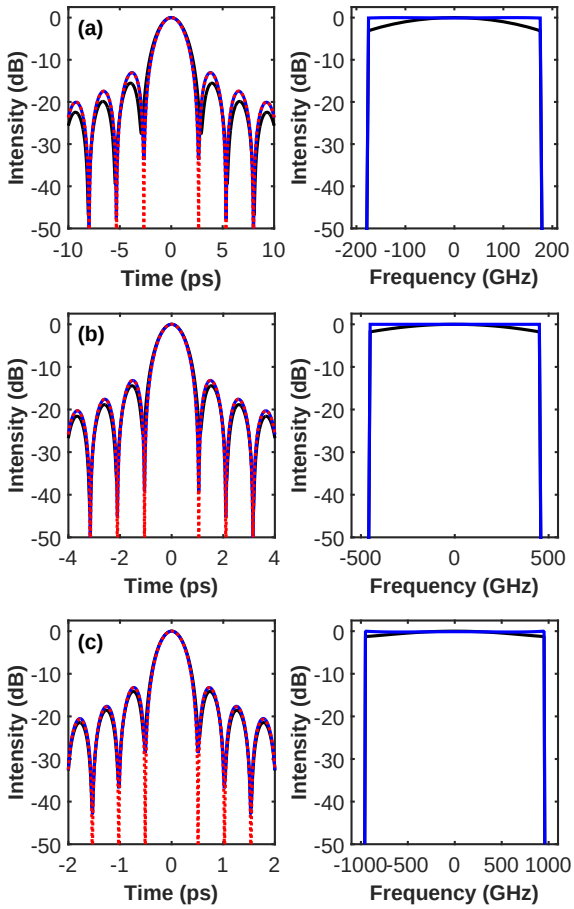

Fig. 2. Temporal (left) and spectral (right) intensity profiles of the output pulse from the laser for different filter bandwidths: (a) $B = 400\,\mathrm{GHz}$ ($\tau_p = 2.5\,\mathrm{ps}$), (b) $B = 1\,\mathrm{THz}$ ($\tau_p = 1\,\mathrm{ps}$), and (c) $B = 2\,\mathrm{THz}$ ($\tau_p = 0.5\,\mathrm{ps}$). The profiles obtained with a flat-top ($\alpha = 0$) spectral pulse shaper (black) are compared with those obtained with a convex Gaussian-top spectral shaper (blue). The correction factor is $\alpha = 6.1,\ 1.1,\ 0.18$ in panels (a), (b), (c), respectively. Also shown are the calculated waveforms according to Eq. (3) (red dotted). A laser without dispersion control in the cavity is modeled.

fiber. Note that the root-mean-square pulse duration is increased by the filter owing to the specific ringing feature (or ripples) on the pulse wings accompanied by the generated Nyquist pulse. The SA decreases the pulse duration and attenuates the pulse ripples. The principle of filtering a pulse in frequency and time due to the large chirp present has already been exploited to achieve new mode-locking regimes in fiber lasers [19], [20]. In the present work, the intended pulse shaping is achieved through enhanced spectral filtering of a nonlinearly spectrally broadened pulse in the cavity [16]. Note that unlike the cavity design presented in [16], here we do not employ an additional passive nonlinear propagation stage in the cavity. Notwithstanding, the spectral broadening in the gain fiber segment is still sufficient to operate a convenient reshaping across a broad range of filter bandwidths. The peak nonlinear phase shift $\phi^{\mathrm{NL}} = \int \mathrm{d}z\, \gamma P_0(z)$ (P_0 is the pulse peak power), which the pulse accumulates in the gain fiber (also known as the B-integral) is approximately 3 rad in the example of Fig. 3. This is accommodated by a spectral breathing factor (defined as the ratio of the spectral FWHM at the input and the output of the filter) of approximately 2. Because the nonlinearly broadened spectrum of the pulse at the output of the fiber is wider than the filter's spectral response and fairly flat within the filter bandwidth, it can be sliced without caring for the

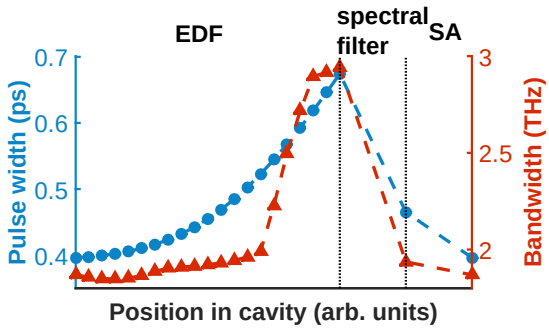

Fig. 3. Evolution of the FWHM temporal (blue circles) and spectral (red triangles) widths of the pulse along the cavity for a flat-top spectral pulse shaper with $B = 2\,\mathrm{THz}$ ($\tau_p = 0.5\,\mathrm{ps}$). A laser without dispersion control in the cavity is modeled.

details of its structure [21]. This is the enabling mechanism for the formation of pulses of the desired temporal shape at the output of the filter, impressed on the pulse by the filter's impulse response.

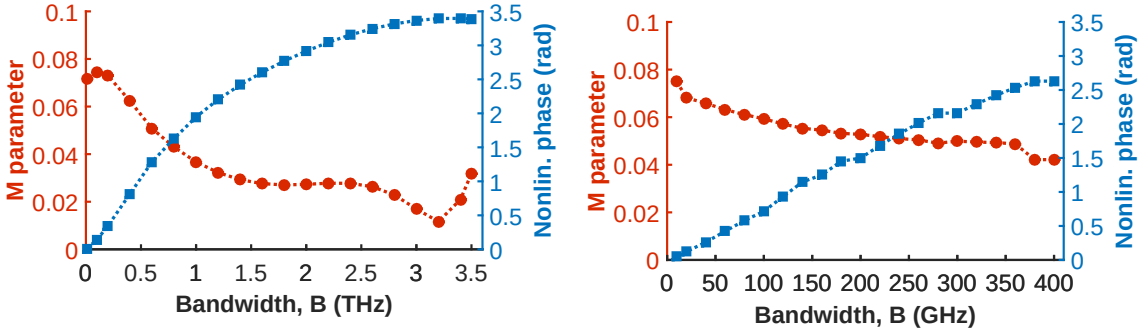

Fig. 4. (Misfit parameter to a sinc shape at the output of the laser (red circles) and peak nonlinear phase shift (blue squares) versus filter bandwidth B for a flat-top spectral pulse shaper and lasers without (left) and with (right) passive nonlinear propagation, in the absence of in-cavity dispersion control.

In order to illustrate the flexibility of the proposed scheme in terms of output spectral bandwidth, we have changed the zero-crossing duration parameter τ_p in the filter's impulse response over a wide range, and assessed the quality of the obtained pulses with the metric $M^2 = \int \mathrm{d}t\,(|\psi|^2 - |\chi|^2)^2 / \int \mathrm{d}t\,|\psi|^4$. Here ψ is the pulse being evaluated, and χ is the theoretical sinc function (Eq. (3)) with the same peak amplitude. In each case, we have verified that the spectrum was close to the ideal rectangular one. In the left panel of Fig. 4, we summarize the results obtained with a flat-top spectral profile applied to the filter and in the absence of in-cavity dispersion control. It is seen that the quality of the generated sinc pulses improves with increasing values of the filter bandwidth, which enable increasingly higher values of the nonlinear phase shift accumulated in the fiber. This confirms that the pulse-shaping mechanism of our laser design requires SPM, and gets stronger with increasing pulse intensity and nonlinear phase shift. The peak nonlinear phase shift accumulated by the pulse, however, saturates to about 3.5 rad in our laser configuration. Above this value, the pulse spectrum after the fiber begins to split and oscillations begin to appear in its central part. It is seen in the left panel of Fig. 4 that sinc-shaped pulses with low M values ($M \leq 0.06$) are obtained over the bandwidth range from a few hundred gigahertz to a few terahertz. At smaller bandwidths, in order to enhance the spectral breathing, hence, the filtering process,

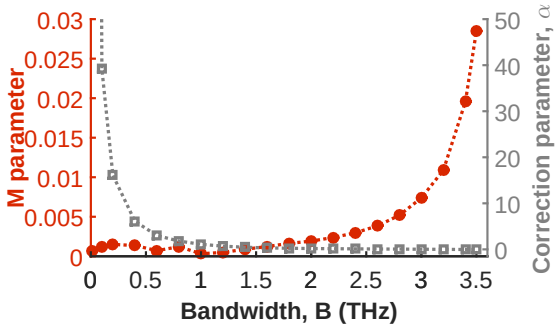

Fig. 5. Misfit parameter to a sinc shape at the output of the laser (red circles) and correction factor α (grey open squares) versus filter bandwidth B for a Gaussian-top spectral pulse shaper and a laser without passive nonlinear propagation, in the absence of in-cavity dispersion control.

more nonlinear pulse propagation is necessary in the cavity. To this end, one may either use a longer gain fiber segment or incorporate a short segment of passive nonlinear fiber into the cavity. In the spirit of prior work on in-cavity spectral enhancement [16], [22], we placed a 20 cm-long segment of highly-nonlinear photonic-crystal fiber ($\beta_2 = 7\,\mathrm{fs}^2/\mathrm{mm}$ and nonlinear coefficient nine times larger than that of the gain fiber) after the gain fiber. As the right panel of Fig. 4 shows, high-quality sinc-shaped pulses were indeed obtained over the bandwidth range from a few ten to a few hundred gigahertz in this case. We confirmed in the simulation that a similar performance was also achieved with 2 m of gain fiber and without passive nonlinear propagation. For larger bandwidths than the upper bounds of the intervals shown in Fig. 4, stable single-pulsing was not possible.

Figure 5 outlines the results obtained for the same laser configuration as that shown in the left panel of Fig. 4, but using now the enhanced spectral filtering method. Misfit values to a sinc pulse shape below 0.03 are possible with this strategy over the full bandwidth range being studied. Remarkably, the misfit parameter is reduced by a factor of more than ten (and even reaching a hundred in some cases) with respect to the rectangular filtering approach for bandwidths between the lower bound of the interval studied (10 GHz) and 2.2 THz. This relaxes the need for large nonlinear phase accumulation or, in other words, large spectral broadening in the fiber section to obtain a fairly flat pulse spectrum within the filter bandwidth. Indeed, a higher degree of concavity of the output spectrum from the fiber stemming from a lower extent of nonlinear spectral expansion can be offset by a higher value of the correction factor α (Fig. 2). The increase of the misfit parameter with increasing bandwidth after approximately 1.5 THz is due to the fact that at such large bandwidths, some structure of the nonlinearly broadened pulse spectrum at the fiber output falls within the filter bandwidth. Such a structure cannot be efficiently cancelled by applying a simple convex function. Consequently, the strength of the corrective spectral shaping approach increasingly diminishes with increasing bandwidth, as it is evident from the misfit parameter increasingly approaching the values obtained with the basic shaping approach. Ultimately, the corrective approach becomes dispensable. However, within such a bandwidth range, the generated sinc pulses with the basic approach are already of very high quality (Fig. 4) and, thus, do not compulsorily require corrections.

We also studied the effect of net cavity dispersion on the quality of the generated Nyquist pulses. The results presented in Fig. 6 show that the tolerance of Nyquist pulse shaping to the cavity dispersion increases with increasing pulse duration, while the dispersion range where the best sinc-shaped pulses are obtained shifts toward increasingly higher values of normal dispersion when the basic rectangular filtering method is employed. Figure 6 also highlights a typical scenario of when a corrective Gaussian-top profile is applied to the filter: when anomalous GVD is added into the cavity, a larger shape correction factor α can compensate for the higher degree of concavity

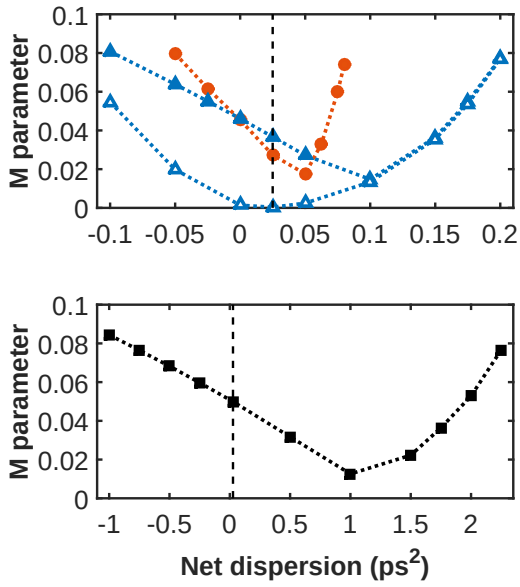

Fig. 6. Misfit parameter to a sinc shape at the output of the laser versus net cavity dispersion for: a flat-top spectral pulse shaper with $B = 2\,\mathrm{THz}$ and a cavity without passive nonlinear propagation (red circles), flat-top (blue triangles) and Gaussian-top (blue open triangles) spectral pulse shapers with $B = 1\,\mathrm{THz}$ and a cavity without passive nonlinear propagation, a flat-top spectral pulse shaper with $B = 300\,\mathrm{GHz}$ and a cavity with passive nonlinear propagation (black squares). The natural dispersion of the cavity is shown by a dashed line.

of the pulse spectrum at the output of the fiber to some extent, and so better quality sinc-shaped pulses can be obtained compared to the basic filtering method. On the contrary, with increasing normal dispersion in the cavity, the pulse spectrum at the output of the fiber acquires an increasing convex feature, which cannot be offset by a concave filter's spectral profile ($\alpha < 0$). Therefore, the improvement in pulse quality brought about by the corrective method using small negative values of α is minimal. Furthermore, we investigated the influence of higher-order dispersion of the gain fiber on the generated sub-picosecond Nyquist pulses. For typical values of the third-order dispersion (TOD) coefficient of the fiber from 50 to $100\,\mathrm{fs}^3/\mathrm{mm}$, we did not observe any appreciable effects of the TOD on the pulses. This indicates that the higher-order dispersion does not limit the operation or performance of our Nyquist laser.

4. Conclusions

We have numerically shown the possibility of directly generating sinc-shaped Nyquist pulses of high quality from a passively mode-locked fiber laser incorporating a simple flat-top spectral filter in the cavity. Pulse shaping in such a laser occurs through filtering of a spectrally nonlinearly broadened pulse in the cavity. We have also shown that the use of a filter's profile with a corrective convex top can compensate for the concavity of the nonlinearly broadened pulse spectrum in the fiber, thereby relaxing the need for large nonlinear phase accumulation. In principle, the corrective spectral shaping approach presented here could be used to synthesize any kind of dissipative solitons in a mode-locked fiber laser with a very high precision. The filtering process being used enables tunability of the output spectral bandwidth over a wide range, up to a few terahertz. The high flexibility of the bandwidth can be of particular interest for photonic assisted technologies such as photonic analog-to-digital conversion or optical sampling. It is also noteworthy that the simplicity of the proposed fiber laser design is appealing for implementation in experiments. It is typical in

optical communications that the availability of a certain technical solution refocuses research on the feasibility of simpler or more cost-efficient versions. From a fundamental standpoint, our work confirms the great potential of the concept of an in-cavity pulse shaper for manipulating and controlling the dynamics of mode-locked fiber lasers and, thus, enabling different mode-locking regimes.

Acknowledgements

The authors would like to acknowledge support by the Leverhulme Trust (grant RPG-278) and the EPSRC Program grant UNLOC (EP/J017582/1).

References

[1] J. G. Proakis and M. Salehi, *Digital Communications*, 5th edn. (McGraw-Hill, 2008).
[2] J. Leuthold and W. Freude, "Optical OFDM and Nyquist multiplexing," in *Optical Fiber Telecommunications V1B*, pp. 381–432, I. P. Kaminov, T. Lee, and A. E. Willner eds. (Elsevier, 2013).
[3] G. C. Valley, "Photonic analog-to-digital converters," *Optics Express*, vol. 15, no. 5, pp. 1955-1982, 2007.
[4] M. Pawlak and E. Rafajlowicz,"On restoring band-limited signals," *IEEE Transanctions on Information Theory*, vol. 40, no. 5, pp. 1490-1503, 1994.
[5] V. R. Supradeepa, C. M. Long, R. Wu, F. Ferdous, E. Hamidi, D. E. Leaird, and A. M. Weiner, "Comb-based radiofrequency photonic filters with rapid tunability and high selectivity," *Nature Photonics*, vol. 6, pp186–194, 2012.
[6] M. Santagiustina, S. Chin, N. Primerov, L. Ursini, and L. Thèvenaz, "All-optical signal processing using dynamic Brillouin gratings," *Scientific Reports*, vol. 3, article number 1594, 2013.
[7] D. Pestov, R. K. Murawski, G. O. Ariunbold, X. Wang, M. Zhi, A. V. Sokolov, V. A. Sautenkov, Y. V. Rostovtsev, A. Dogariu, Y. Huang, and M. O. Scully, "Optimizing the laser-pulse configuration for coherent Raman spectroscopy," *Science*, vol. 316, no. 5822, pp. 265–268, 2007.
[8] S. Preußler, K. Jamshidi, A. Wiatrek, R. Henker, C.-A. Bunge, and T. Schneider, "Quasi-light-storage based on timefrequency coherence," *Optics Express*, vol. 17, no. 18, pp. 15790-15798, 2009.
[9] M. Nakazawa, T. Hirooka, P. Ruan, and P. Guan, "Ultrahigh-speed "orhtogonal" TDM transmission with an optical Nyquist pulse train," *Optics Express*, vol. 20, no. 2, pp. 1129–1140, 2012.
[10] A. Vedadi, M. A. Shoaie, and C.-S. Brès, "Near-Nyquist optical pulse generation with fiber optical parametric amplification," *Optics Express*, vol. 20, no. 26, pp. B558–B565, 2012.
[11] M. A. Soto, M. Alem, M. A. Shoaie, A. Vedadi, C.-S. Brès, L. Thévenaz, and T. Schneider, "Optical sinc-shaped Nyquist pulses of exceptional quality," *Nature Communications*, vol. 4, article number 3898, 2013.
[12] S. Cordette, A. Vedadi, M. A. Shoaie, and C.-S. Brès, "Bandwidth and repetition rate programmable Nyquist sinc-shaped pulse train source based on intensity modulators and four-wave mixing," *Optics Letters*, vol. 39, no. 23, pp. 6668–6671, 2014.
[13] M. Nakazawa, M. Yoshida, and T. Hirooka, "The Nyquist laser," *Optica*, vol. 1, no. 1, pp. 15–22, 2014.
[14] J. Schröder, T. D. Vo, and B. J. Eggleton, "Repetition-rate-selective, wavelength-tunable mode-locked laser at up to 640 GHz," *Optics Letters*, vol. 34, no. 24, pp. 3902–3904 (2009).
[15] J. Schröder, S. Coen, T. Sylvestre, and B. J. Eggleton, "Dark and bright pulse passive mode-locked laser with in-cavity pulse-shaper," *Optics Express*, vol. 18, no. 22, pp. 22715–22721, 2010.
[16] S. Boscolo, C. Finot, H. Karakuzu, and P. Petropoulos, "Pulse shaping in mode-locked fiber lasers by in-cavity spectral filter," *Optics Letters*, vol. 39, no. 3, pp. 438–441, 2014.
[17] F. Ö. Ilday, J. R. Buckley, W. G. Clark, and F. W. Wise, "Self-similar evolution of parabolic pulses in a laser," *Physical Review Letters*, vol. 92, no. 21, pp. 213902(4), 2004.
[18] M. Roelens, S. Frisken, J. Bolger, D. Abakoumov, G. Baxter, S. Poole, and B. Eggleton, "Dispersion trimming in a reconfigurable wavelength selective switch," *Journal of Lightwave Technology*, vol. 26, no. 1, pp. 73–78, 2008.
[19] B. Oktem, C. Ülgüdür, and F. Ö. Ilday, "Soliton-similariton fibre laser," *Nature Photonics*, vol. 4, pp. 307–311, 2010.
[20] W. H. Renninger, A. Chong, and F. W. Wise, "Self-similar pulse evolution in an all-normal-dispersion laser," *Physical Review A*, vol. 82, no. 2, pp. 021805(4), 2010.
[21] C. Finot and G. Millot, "Synthesis of optical pulses by use of similaritons," *Optics Express*, vol. 12, no. 21, pp. 5104–5109, 2004.
[22] A. Chong, H. Liu, B. Nie, B. G. Bale, S. Wabnitz, W. H. Renninger, M. Dantus, and F. W. Wise, "Pulse generation without gain-bandwidth limitation in a laser with self-similar evolution," *Optics Express*, vol. 20, no. 13, pp. 14213–14220, 2012.